Ab initio band structure calculations of the low-temperature phases of Ag2Se, Ag2Te and Ag3AuSe2

Fang, C.M.; Groot, R.A. de; Wiegers, G.A.

Published in:
Journal of Physics and Chemistry of Solids

DOI:
10.1016/S0022-3697(01)00160-3

Publication date:
2002

ELSEVIER

Journal of Physics and Chemistry of Solids 63 (2002) 457–464

JOURNAL OF PHYSICS AND CHEMISTRY OF SOLIDS

www.elsevier.com/locate/jpcs

Ab initio band structure calculations of the low-temperature phases of Ag_2Se, Ag_2Te and Ag_3AuSe_2

C.M. Fang[a,b,*], R.A. de Groot[a,c], G.A. Wiegers[c]

[a]*Electronic structure of Materials, Research Institute for Materials, Toernooiveld 1, 6525 ED Nijmegen, The Netherlands*
[b]*Laboratory of Solid State and Material Chemistry, Technical University of Eindhoven, Post-bus 513, 5600 MB Eindhoven, The Netherlands*
[c]*Inorganic Solid State Chemistry Laboratory, Materials Science Center, University of Groningen, Nijenborgh 4, 9747 AG, Groningen, The Netherlands*

Received 10 January 2001; accepted 14 June 2001

Abstract

Ab initio band structure calculations were performed for the low-temperature modifications of the silver chalcogenides β-Ag_2Se, β-Ag_2Te and the ternary compound β-Ag_3AuSe_2 by the local spherical wave (LSW) method. Coordinates of the atoms of β-Ag_2Se and β-Ag_3AuSe_2 were obtained from refinements using X-ray powder data. The structures are characterized by three, four and five coordinations of silver by the chalcogen, a linear coordination of gold by Se, and by metal–metal distances only slightly larger than in the metals. The band structure calculations show that β-Ag_3AuSe_2 is a semiconductor, while β-Ag_2Se and β-Ag_2Te are semimetals with an overlap of about 0.1–0.2 eV. The Ag 4d and Au 5d states are strongly hybridized with the chalcogen p states all over the valence bands. β-Ag_2Se and β-Ag_2Te have a very low DOS in the energy range from about −0.1 to +0.5 eV. The calculated effective mass β-Ag_2Se is about 0.1–0.3 m_e for electrons and 0.75 m_e for holes, respectively.

Keywords: A. Chalcogenides; C. X-ray powder diffraction; C. Ab initio calculations; D. Crystal structure; D. Electronic structure

1. Introduction

Recently, an unusually large and positive magnetoresistance (MR) was reported [1] for the low-temperature (β) phases of Ag_2Se and Ag_2Te, and for thin films of Ag_2Te [2]. These compounds are non-magnetic. To understand the origin of the MR in these compounds knowledge of electronic structure becomes important.

The silver chalcogenides have been studied, in particular because of their high ionic conductivity (of Ag^+) in the high temperature (α) structures, in addition to an electronic conductivity, which is much larger than the ionic conductivity in the case of Ag_2Se and Ag_2Te, but is comparable in magnitude for Ag_2S.

The low-temperature phases β-Ag_2Se and β-Ag_2Te are known as the minerals naumanite and petzite, respectively. These compounds show a transition at rather low temperatures from the ordered β structure to the disordered α structure. The transition temperature is 139°C for Ag_2Se and 145°C for Ag_2Te. The high ionic conductivity in the α phase of Ag_2Se and Ag_2Te is due to a statistical distribution of the silver atoms in an ordered chalcogen sublattice (body centered cubic for Ag_2Se and face centered cubic for Ag_2Te), together with a low activation energy for diffusion of the silver ions. In the system Ag–Au–Se, there is an ordered compound β-Ag_3AuSe_2 with a transition to a disordered α phase at 267°C.

The structures of β-Ag_2Se and β-Ag_2Te are characterized by silver in different types of coordination by chalcogen, and by Ag–Ag distances that are only slightly larger than in the metals. β-Ag_3AuSe_2 has gold in a linear coordination by selenium, silver in an approximately tetrahedral coordination by Se and short metal–metal distances.

The electrical transport properties of Ag_2Se and Ag_2Te have been extensively studied. A review up to 1971 is given in Ref. [3]. In relation to the results of the band structure calculations it is important to notice that both compounds are small gap semiconductors (about 70 meV for Ag_2Se and 20–50 meV for Ag_2Te). The deviation from stoichiometry

* Corresponding author. Tel.: +31-4024-73041.
E-mail address: c.m.fang@tue.nl (C.M. Fang).

0022-3697/02/$ - see front matter
PII: S0022-3697(01)00160-3

(they have a relatively large range of homogeneity, $Ag_{2+\delta}X$) determines strongly the electronic conductivity and activation energy. The mobility of electrons and holes is high and they have a small effective mass. The concentration of electron-carriers is about 3×10^{18} cm^{-3} [4].

The electrical transport properties of β-Ag_3AuSe_2 have scarcely been investigated. Wiegers [5] found it to be a p-type semiconductor with a gap of about 1.0 eV. The Seebeck coefficient α is positive. Diffuse reflection spectra revealed an energy gap of about 0.9 eV [5].

In this paper, band structure calculations are reported for β-Ag_2Se, β-Ag_2Te and β-Ag_3AuSe_2 using density functional theory (DTF) within the local density approximation (LDA). Lattice parameters and coordinates of β-Ag_2Te are from an accurate single crystal refinement by van der Lee and de Boer [6]. For β-Ag_2Se and β-Ag_3AuSe_2, the coordinates were obtained from refinements using X-ray powder data, which are also described in the present paper.

2. Crystal structure refinements

The structure of the low-temperature (β) phase of Ag_2Se has been subject of many studies by electron and X-ray diffraction. Most X-ray diffraction studies agree in an orthorhombic unit cell with the lattice parameters: $a = 4.3$, $b = 7.05$ and $c = 7.8$ Å. Electron diffraction revealed, besides the orthorhombic unit cell, a similar triclinic unit cell with α, β, and γ deviating 1–2° from 90° [7]. In a recent electron diffraction study by Kaito et al. [8], the triclinic cell was found for samples with excess selenium, while orthorhombic symmetry was found for stoichiometric Ag_2Se. A structure determination of β-Ag_2Se was published in 1971 by one of the present authors (G.A.W. [9]). The unit cell dimensions of the orthorhombic cell are: $a = 4.333(2)$, $b = 7.062(4)$, $c = 7.764(4)$ Å, in good agreement with those found by Conn and Taylor [10]. Refinement in space group $P2_12_12_1$ using the integrated intensities of all reflections down to $d = 1.41$ Å was performed [9] using the program T53C written by Rieveld [11]. Coordinates in Ref. [9] were given in a non-standard setting of the space group; note: to get them in standard setting 1/4 must be added to the x and y coordinates. The agreement between observed and calculated intensities was $R(F^2) = 8.3\%$. Standard deviations in the coordinates are 0.002–0.004. Powder diffraction data are given in Ref. [9] and in JCPDS (24-1041). More accurate coordinates for the band structure calculation were obtained from powder data (Philips diffractometer, Cu K_α radiation) using the program FULLPROF for profile refinement [12]. The results are listed in Table 1. The coordinates of the previous refinement [9] are within s.d. equal to the present one.

Compounds Ag_3AuTe_2 and Ag_3AuSe_2 are known as the minerals petzite and fischesserite, respectively. Frue [13] determined the structure of petzite by single crystal diffraction. The compound is cubic, $a = 10.38$ Å. The atoms are at special sites of space group $I4_132$: 8a (1/8, 1/8, 1/8) for Au, 24f (x, 0, 1/4; $x = 0.365$) for Ag and 16e (x, x, x; $x = 0.266$) for Te.

Table 1
Results of a profile refinement of the structure of β-Ag_2Se, with $a = 4.3363(6)$ Å, $b = 7.0675(9)$ Å, $c = 7.767(1)$ Å; space group $P2_12_12_1$. R(Bragg) = 9.2%, $R(F) = 6.0\%$; Rp = 10.1%, Rwp = 13.4%. Standard deviations are in parentheses

Atom	x	y	z
Ag(1)	0.3551(12)	0.6146(7)	0.4533(6)
Ag(2)	0.9812(10)	0.2781(8)	0.3615(7)
Se	0.6139(13)	0.4931(10)	0.1512(9)

Ag_3AuX_2 (X = Se and Te) can be synthesized by interaction between Ag_2X precipitates and thio–gold(I) complexes [14]. Using X-ray powder diffraction, Messien and Baiwir [15] found that Ag_3AuSe_2 prepared in this way is isostructural with Ag_3AuTe_2. The unit cell constant is 9.95 Å, and the x coordinates of Ag and Se were found to be 0.366 and 0.274, respectively (standard deviations were not given). The mineral fischesserite was studied by Johan et al. [16]. They found $a = 9.967$ Å (powder pattern in JCPDS 25-0367).

Ag_3AuSe_2 and Ag_3AuTe_2 can also be prepared from the elements [16,17]. Integrated intensities (powder diffractometer, Cu K_α) measured in a study of the electrical transport properties of the system $Ag_{2-x}Au_xSe$ by one of the present authors [5] were used for a refinement with the integrated intensities option of FULLPROF [12]. The refinement confirmed the results of Messien and Baiwir [15]. The unit cell constant $a = 9.9789(7)$ Å, the space group $I4_132$; x of Ag at 24f is 0.3745(12), x of Se at 16e is 0.2676(11); $R(F^2) = 7.2\%$. The powder pattern is given in Table 2.

3. Discussion of the structures

Interatomic distances are given in Table 3. It is seen that besides the metal–chalcogen distances corresponding to bonding there are metal–metal distances as short as in pure metals. Both β-Ag_2Se and β-Ag_2Te have two types of silver atoms in their structure. The two types of silver have different coordination by chalcogen atoms; Ag(1) of β-Ag_2Se has approximately tetrahedral coordination with Ag(1)–Se distances 2.660–2.871 Å; Ag(2) has trigonal–pyramidal (close to triangular) coordination by Se with Ag(2)–Se distances of 2.674, 2.741 and 2.802 Å and two more Se atoms at distances of 3.275 and 3.540 Å. The Ag–Ag distances are 2.97–3.34 Å, somewhat larger than those in the metal (2.89 Å). In β-Ag_2Te, both types of Ag atoms have a four-fold coordination by Te. The Ag–Ag distances range from 2.84 to 3.13 Å.

The chalcogen packing is distorted body-centered cubic for β-Ag_2Se and distorted face-centered cubic for β-Ag_2Te.

Table 2
X-ray powder diffraction data (Cu K_α) of β-Ag_3AuSe_2 with space group $I4_132$, $a = 9.9789(7)$ Å. Calculated intensities are from FULLPROF refinement

h k l	*d*(calc.) (Å)	*I*(obs.)	*I*(calc.)
1 1 0	7.0561	320	309
2 1 1	4.0739	10	9
2 2 0	3.5281	15	18
3 1 0	3.1556	100	97
2 2 2	2.8807	150	156
3 2 1	2.6670	1000	972
4 0 0	2.4947	10	9
3 3 0/4 1 1	2.3520	180	81/93
4 2 0	2.2313	250	308
3 3 2	2.1275	4	3
4 2 2	2.0369	320	297
4 3 1/5 1 0	1.9570	220	116/95
5 2 1	1.8219	300	266
4 4 0	1.7640	70	79
5 3 0/4 3 3	1.7114	35	18/8
4 4 2	1.6632	4	0
5 3 2/6 1 1	1.6188	20	17/1
6 2 0	1.5778	2	1
5 4 1	1.5398	10	12
6 2 2	1.5044	70	79
6 3 1	1.4713	120	128
4 4 4	1.4403	90	78
5 3 4/7 1 0/5 5 0	1.4112	90	44/34/1
6 4 0	1.3838	70	55
6 3 3/5 5 2/7 2 1	1.3580	13	2/1/11
6 2 4	1.3335	110	115
7 3 0	1.3103	1	1
7 3 2/6 5 1	1.2673	210	102/116
8 0 0	1.2474	90	91

In β-Ag_2Se, there is an almost planar arrangement of Se atoms perpendicular to the *b*-axis at $y = 0$ and 1/2. The Ag(1) atoms lie somewhat above and below these planes (at $y = 0.6146$ and 0.3854) while the Ag(2) atoms (at $y = 0.2781$ and 0.2219) lie half way between these planes of Se. In β-Ag_2Te, two mixed layers of Ag(2)–Te followed by one Ag(1) layer can be distinguished (see Fig. 1 in Ref. [5]). Chupprakov and Dahmen [2] remarked that this compound in this way might be considered as a 'natural multilayer'.

Silver in β-Ag_3AuSe_2 has approximately tetrahedral coordination by Se; gold is linearly coordinated by Se. The metal–metal (Ag–Ag, Ag–Au) distances (3.05 Å) are somewhat larger than in the pure metals (2.89 Å). The Au–Au distances are 3.53 Å, as listed in Table 3.

4. Band structure calculations

Ab initio band structure calculations were performed with the localized spherical wave (LSW) method [18] using a scalar-relativistic Hamiltonian. We used local-density exchange-correlation potentials [19] inside space-filling, and therefore overlapping spheres around the atomic constituents. The self-consistent calculations were carried out including all core electrons. We performed iterations with about 1300 *k*-points distributed uniformly in an irreducible part of the Brillouin zone (BZ), corresponding to a volume of the BZ per *k*-point of less than 1×10^{-5} Å^{-3}. Self-consistency was assumed when the changes in the local partial charges in each atomic sphere decreased to the order of 1×10^{-5}.

In the construction of the LSW basis [18], the spherical waves were augmented by solutions of the scalar-relativistic radial equations indicated by the atomic symbols 4s, 4p and 4d; and 5s, 5p and 4d; 5s 5p and 5d; and 6s, 6p and 5d for Se, Ag, Te and Au, respectively. The internal *l* summation used to augment a Hankel function at surrounding atoms, was extended to $l = 3$, resulting in the use of 4f orbitals for Se, Ag and Te, and 5f for Au. Because the crystals are not very densely packed, it is necessary to include empty spheres (Va) in the calculations. The functions 1s and 2p, and 3d as an extension were used for the empty spheres. The input parameters for calculations are listed in Table 4.

Table 3
Interatomic distances in (a) β-Ag_2Se, (b) β-Ag_2Te [6] and (c) β-Ag_3AuSe_2; distances are in Å

(a)					
Ag(1)–Se	2.660	2.739	2.799	2.871	
Ag(2)–Se	2.674	2.741	2.802	3.275	3.540
Ag(1)–Ag(1)	2.982	2.982			
Ag(2)–Ag(2)	3.081	3.081			
Ag(1)–Ag(2)	2.966	3.336	3.072	3.173	
(b)					
Ag(1)–Te	2.877	2.895	2.965	3.016	
Ag(2)–Te	2.842	2.905	3.011	3.034	
Ag(1)–Ag(1)	2.841	3.010			
Ag(2)–Ag(2)	3.053				
Ag(1)–Ag(2)	3.061	3.133	2.909		
(c)					
Ag–Se	2.73	2.73	2.88	2.88	
Au–Se	2.47	2.47			
Ag–Ag	3.05	3.05	3.06	3.06	
Au–Au	3.53	3.53	3.53		
Ag–Au	3.05	3.95			

5. Electronic structure of β-Ag_2Se and β-Ag_2Te

Fig. 1(a) and (b) show the Brilloun zones for β-Ag_2Se, and β-Ag_2Te, respectively. Some calculated results (electronic configurations) are given in Table 4. There are about 0.57 electrons in Va1 and 0.50 electrons in Va2 for β-Ag_2Se, and 0.25 electrons in Va1 and 0.38 electrons in Va2 for β-Ag_2Te. We remark that not too much significance should be attributed to differences in charge and orbital

Table 4
Input parameters (coordinates of atoms and empty spheres (Va), Wigner–Seitz radii (R_{WS})) and calculated electronic configurations. WP represents the Wyckoff position

WP	Coordinates	R_{WS} (Å)	Electronic configuration
β-Ag_2Se: lattice parameters listed in Table 1			
Ag1	4a (0.3551, 0.6146, 0.4533)	1.447	[Kr] $4d^{9.31}5s^{0.40}5p^{0.34}4f^{0.03}$
Ag2	4a (0.9812, 0.2781, 0.3615)	1.447	[Kr] $4d^{9.32}5s^{0.40}5p^{0.30}4f^{0.03}$
Se	4a (0.6139, 0.4931, 0.1512)	1.768	([Ar] $3d^{10}$) $4s^{1.92}3p^{4.29}4d^{0.40}4f^{0.18}$
Va1	4a (0.6110, 0.3424, 0.8746)	1.172	$1s^{0.28}$ $2p^{0.21}$ $3d^{0.08}$
Va4	4a (0.4411, 0.3296, 0.3953)	1.059	$1s^{0.26}$ $2p^{0.17}$ $3d^{0.07}$
β-Ag_2Te: monoclinic, space group $P2_1/c$[6], $a = 8.164$, $b = 4.468$, $c = 8.977$ Å, $\beta = 124.16^{o}$			
Ag1	4e (0.1880, 0.1507, 0.3710)	1.471	[Kr] $4d^{9.37}5s^{0.48}5p^{0.43}4f^{0.03}$
Ag2	4e (0.3327, 0.8383, 0.9957)	1.471	[Kr] $4d^{9.37}5s^{0.42}5p^{0.32}4f^{0.02}$
Te	4e (0.2718, 0.1584, 0.2425)	1.961	([Kr] $4d^{10}$)$5s^{1.91}3p^{4.17}5d^{0.50}4f^{0.25}$
Va1	4e (0.4450, 0.8400, 0.8040)	1.151	$1s^{0.17}$ $2p^{0.13}$ $3d^{0.04}$
Va2	4e (0.0850, 0.7630, 0.9810)	0.954	$1s^{0.22}$ $2p^{0.12}$ $3d^{0.04}$
β-Ag_3AuSe_2: cubic, space group $I4_132$, $a = 9.9789$ Å			
Au	8a (0.1250, 0.1250, 0.1250)	1.468	[Xe] $4f^{14}$ $5d^{8.91}6s^{0.71}6p^{0.32}5f^{0.03}$
Ag	24f (0.3745, 0.0000, 0.2500)	1.468	[Kr] $4d^{9.37}5s^{0.44}5p^{0.36}4f^{0.03}$
Se	16e (0.2676, 0.2780, 0.2780)	1.714	([Ar] $3d^{10}$) $4s^{1.88}4p^{3.98}4d^{0.34}4f^{0.15}$
Va1	12d (0.6250, 0.0000, 0.2500)	1.230	$1s^{0.20}$ $2p^{0.21}$ $3d^{0.09}$
Va2	24g (0.1250, 0.0844, 0.3344)	1.108	$1s^{0.32}$ $2p^{0.24}$ $3d^{0.09}$

configurations, as these numbers are dependent on the Wigner–Seitz radii, and the presence of empty spheres. The partial and total densities of states (DOS), and the energy bands along the high-symmetry directions in the Brillouin zones are shown in Figs. 2–5.

In β-Ag_2Se the lowest bands (Figs. 2 and 3), ranging from −13.58 to −12.80 eV (Fermi level is at zero eV), consist mainly of Se 4s orbitals. The next bands, ranging from −6.28 up to about the Fermi level (the valence band) are composed mainly of Ag 4d and Se 4p states. The contribution of other states is at least one order of magnitude smaller. The partial density of Se 4p states has higher values at the bottom of the valence band and near the Fermi level. That is quite similar to the partial density of O 2p states in Ag_2O [20] and that of the S 3p states in β-Ag_2S [21], in contrast to the quite flat shape of the density of the Te 5p states in β-Ag_2Te (see Figs. 2–5). There are holes in the Se 4p states, which extend to above the Fermi energy.

The partial DOS of the Ag 4d states show a high density at the energy range between about −6.0 eV to −3.0 eV with quite localized character. However, there are also some Ag 4d states showing delocalization. They exist through the valence band, which is different from the quite localized character of the Ag 4d states in the metal [22]. There is a small, but important, contribution of Ag 5s states all over the valence band, especially at the bottom of the valence band. The Ag 5s states are strongly hybridized with Se 4p orbitals.

The total DOS at the Fermi level is very low (about 0.1–0.2 states/eV). In fact, the DOS is also very low from −0.1 to 1.0 eV, which can be seen in the dispersion of the energy bands: there are just two bands from about 1.0 eV down to below the Fermi level. The two bands from the conduction band, composed of Ag 5s and Se 4p states, cross the Fermi level at X–Γ–Y, while two bands consisting of Se 4p states from the valence band cross the Fermi level along the same line. Therefore, β-Ag_2Se is a semimetal with an overlap of about 0.15 eV. Both the top of the valence band and the bottom of the conduction band are at or near Γ, as shown in Fig. 3.

The electronic structure of β-Ag_2Te is similar to that of β-Ag_2Se. However, there are some differences. The Te 5s bands range from −12.13 to −11.22 eV, about 1.5 eV higher than Se 4s of β-Ag_2Se. The gap between the Te 5s and Te 5p(Ag 4d, 5s) is 4.81 eV. The valence band is composed mainly of Ag 4d and Te 5p states. At the bottom of the valence band, there is a peak consisting of Ag 5s hybridized with Te 5p. The partial DOS of Te 5p states have a flat shape over the valence band, which indicates covalency. In fact, the shape of X np states changes gradually from high densities at the bottom and the top of the valence band to a more flat form from X = O to Te (Ag_2O [20], β-Ag_2S [21]), due to the change in the ionicity of the Ag–X bond. The partial density of Ag 4d states for Ag1 is different from that of Ag2. Ag1 has a feature between −6.4 and −4.0 eV, while Ag2 has a peak located at about −4.2 eV. Such a difference can be explained by the existence of metal–metal bonds. There are two short Ag1–Ag1 distances: one is 3.009 Å, the other is 2.841 Å, which is even shorter than the Ag–Ag distance in the metal (2.89 Å), while Ag2 has only one nearest Ag2 neighbor with Ag2–Ag2 distance of 3.053 Å (Table 4). The dispersion curves of

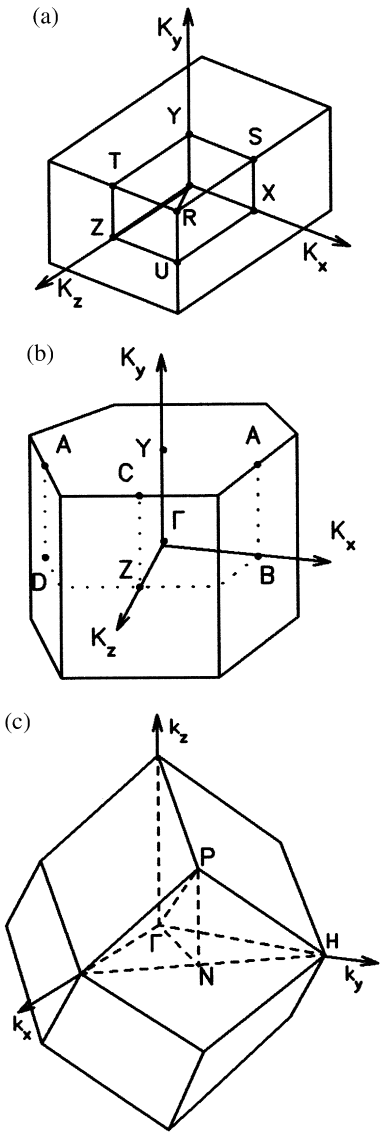

Fig. 1. Brillouin zone and high symmetry points of β-Ag_2Se with a simple orthorhormbic structure (a), β-Ag_2Te with a monoclinic structure (b), and β-Ag_3AuSe_2 with a body-centered cubic structure (c).

β-Ag_2Te and β-Ag_2Se show little anisotropy in different directions, as shown in Figs. 3 and 5.

The DOS at and above the Fermi level for β-Ag_2Te is, similar to Ag_2Se, very low (about 0.1 states/eV). The dispersion curves show that there are bands crossing the Fermi level from both the conduction and the valence bands, with a small overlap (about 0.1 eV, Fig. 5). The top of the valence band is at Γ and along the Γ–Y line, as shown in Fig. 5. The bottom of the conduction band is around Γ.

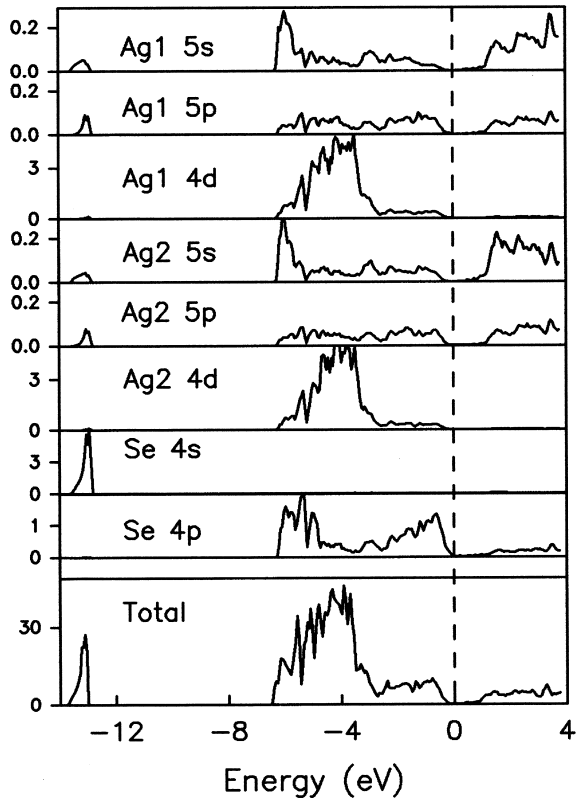

Fig. 2. Partial and total density of states for β-Ag_2Se. The Fermi level is at zero eV, the same in Figs. 4 and 6.

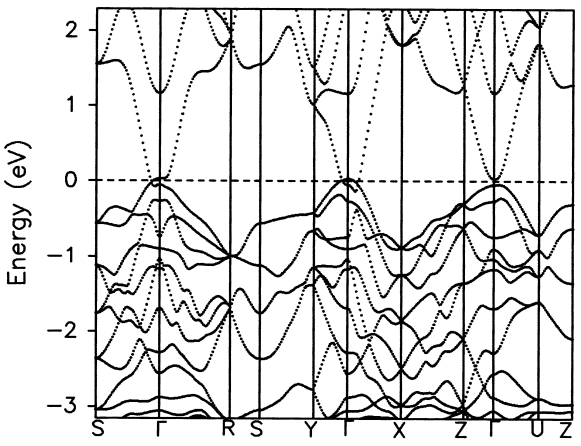

Fig. 3. Dispersion of the energy bands for β-Ag_2Se near the Fermi level.

6. Electronic structure of β-Ag_3AuSe_2

The calculated electronic configurations are included in Table 4. Again we remark that not too much significance should be attributed to differences in charge and orbital

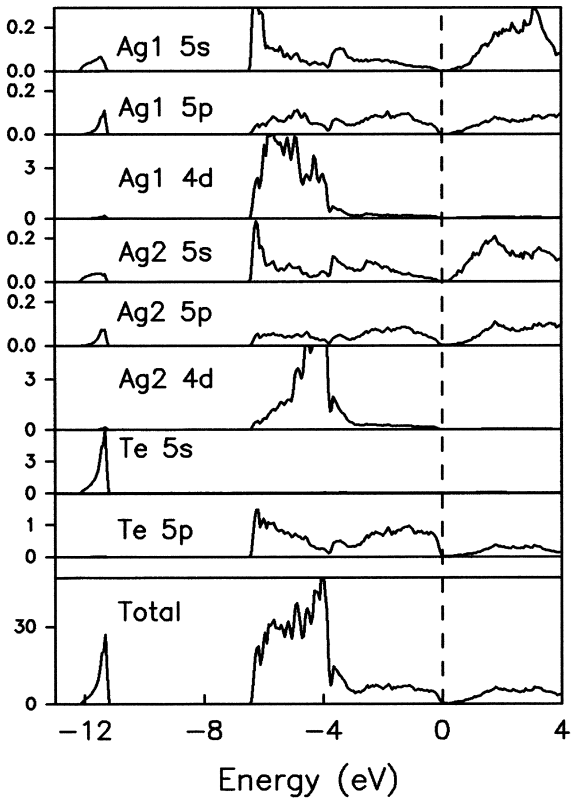

Fig. 4. Partial and total density of states of β-Ag_2Te.

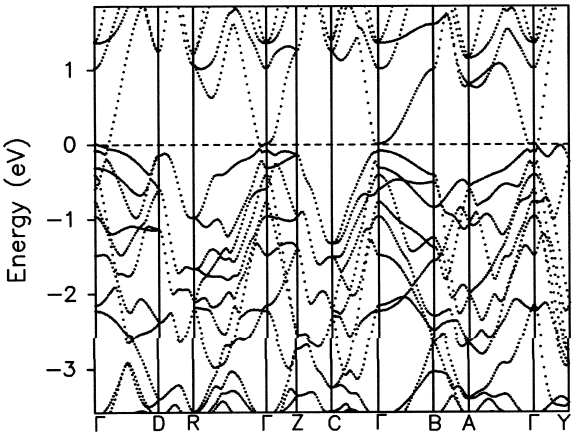

Fig. 5. Dispersion of the energy bands for β-Ag_2Te near the Fermi level.

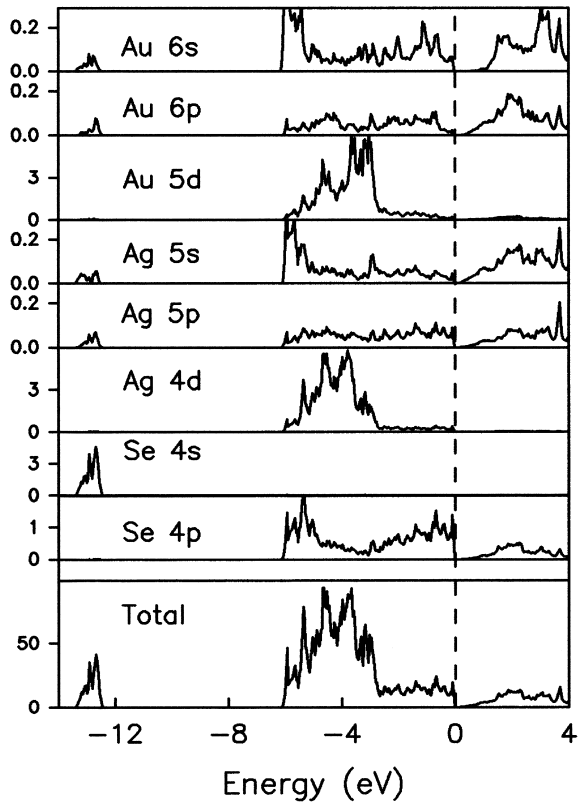

Fig. 6. Partial and total density of states for β-Ag_3AuSe_2.

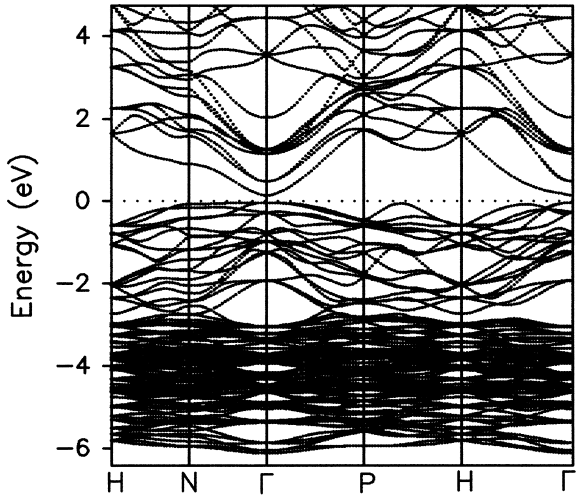

Fig. 7. Dispersion of the energy bands for β-Ag_3AuSe_2 near the Fermi level.

configurations. The BZ is included in Fig. 1c. The partial and total densities of states (DOS), and the dispersion curve of the energy bands along the high-symmetry directions in the BZ are shown in Figs. 6 and 7, respectively.

The density of states for β-Ag_3AuSe_3 is approximately similar to that of β-Ag_2Se. The Se 4s band ranges from −13.35 to −12.45 eV respective to the Fermi energy at the top of the valence band. The valence band, ranging from −6.13 eV to the Fermi level, is composed of Se 4p, Au 5d and Ag 4d states, with some s and p contributions. There is a small peak at the bottom of the valence band,

mainly consisting of the s states of the metals and Se 5p states. The metals' d states appear in two parts: one part is in the energy range from about −6.0 to −3.0 eV with localized character, corresponding to small dispersion as shown in Fig. 7. The localized Au 5d band has a high density in the energy range from about −3.0 to −4.0 eV, and the localized Ag 4d band has a high density in the energy range from about −3.8 to −4.8 eV. The other part of the metal d states is all over the valence band. It should be noted that in the metals the d band of Ag ranges from about −6.6 to −2.6 eV, and of Au 5d from −7.5 to −1.6 eV [22]. As shown in Fig. 7, the top of the valence band is at Γ. The top of the valence band along the Γ–N, Γ–H and P–H lines are close to the top of the conduction bands at Γ. The bottom of the conduction band is at Γ. There is a direct gap of about 0.2 eV at Γ.

7. Discussions and conclusions

Electrical transport and optical property measurements for β-Ag_2Se and β-Ag_2Te showed a wide variation of conductivity and activation energy depending on the thermal history and stoichiometry. For β-Ag_2Se, the energy gap ranges from about 0.045 to 0.11 eV [3,4,23,24]. The transport measurements reported by Xu. et al. [1] indicated that the energy gap is about 0.005 eV for β-Ag_2Se and 0.009 eV β-Ag_2Te. Junod [4] found a band gap of 0.07 eV for β-Ag_2Se, while a reinvestigation by Simon et al. [29] yielded a gap of 0.04 eV. Our calculations show that both β-Ag_2Se and β-Ag_2Te are semimetals with an overlap about 0.1 to 0.2 eV. We remark that our calculations based on the LDA [25], cannot exclude the possibility that both β-Ag_2Se and β-Ag_2Te are small gap semiconductors. For the same reason, the calculated band gap for β-Ag_3AuSe_2 is about 0.2 eV, also smaller than experimental (about 1.0 eV) [5].

Xu et al. [1] found a large, positive MR in $Ag_{2+\delta}Se$ and $Ag_{2+\delta}Te$ with a linear dependence on applied magnetic field. Usually, a quadratic dependence on the filed is expected, i.e. in the case of narrow band gap semiconductors with light and heavy charge carriers of the same sign. Here, we calculate the effective mass m^* of conducting electrons or holes from the dispersion curves of β-Ag_2Se using the formula: $m^* = \{(\partial^2 E/\partial k^2)/\hbar^2\}^{-1}$, where, E is the energy in the dispersion in k space, $\hbar$ the Planck constant. The effective masses for the conducting electrons and holes were obtained by corrections to the LDA. That is, the conduction bands and the valence bands were separated due to the reason that in general the LDA underestimates the energy gap, as stated above. We expect that the corrections to the LDA will not significantly modify the effective masses. In this way, we obtained an effective mass for conduction electrons of 0.28 m_e for the conduction band along the Z–Γ line, and 0.12 m_e for the band along the Γ–X line, as shown in Fig. 3. The effective mass of the conduction holes is about 0.75 m_e along the Y–Γ line. The values (0.1–0.3 m_e) for the effective mass of electrons are in line with experimental data (0.12 m_e [24,26], 0.17 m_e [24,27]). Junod [4] found 0.32 m_e and 0.54 m_e for electrons and holes, respectively. They are larger than that (0.08 m_e) from the semi-empirical calculation [28]. These data were obtained from band structure calculations neglecting spin–orbital interaction. However, because of the low symmetry of the crystal structures involved (orthorhombic and monoclinic) a sizable orbital quenching persists even at Γ and the influence of spin–orbital interaction can be expected to be strongly reduced as compared with cubic systems with comparable composition. The measurements were performed with samples of δ in the range of 0.01–0.33 [1], far outside the homogeneity region of the phases ($\delta < 10^{-3}$ [3]). Subsequent work by Ogorelec et al. [30] did show a quadratic dependence on the magnetic field, but substantially reduced scale as compared with that by Xu et al. [1]. The composition of the samples was not specified in Ref. [30].

Large, positive MRs were reported on inhomogeneous systems by Thio et al. [31,32]. However, here a quadratic dependence on applied field was also found, unlike the observation of Xu et al. [1].

A theoretical paper by Abrikosov [33], does lead to a MR linear dependence on applied field. In this theory, two ingredients can in principle be compared with the present calculations: a direct bandgap of negligible size and a linear dispersion of the electron states in the doped samples. Since our calculations employ the LDA, a negative gap is found with overlapping. Both conduction minima and valence maxima are at Γ. Since better-than-LDA approximations primarily correct the size of the bandgap [25], it is expected that a direct bandgap at Γ exists in the real material. A linear dispersion on a microscopic scale cannot, however, be derived from the present LDA calculation.

In conclusion, using powder diffraction we refined the coordinates of the atoms in the crystal structure of the low-temperature phases β-Ag_2Se and β-Ag_3AuSe_2. Ab initio band structure calculations show that in the compounds β-Ag_2AuSe_2 and β-Ag_2X (X = Se, Te) the Ag 4d (Au 5d) states show strong interaction with the Se 4p (Te 5p) orbitals. The calculations show that β-Ag_2AuSe_2 is a semiconductor with an energy gap of about 0.2 eV, while there is a small overlap between the conduction and valence bands for β-Ag_2X (X = Se, Te). In the energy range from below the Fermi energy to about 0.5 to 1.0 eV the density of states is very low. The interaction between Ag and Se (Te) shows covalent character. The effective masses of conducting electrons and holes for Ag_2Se are 0.12–0.3 m_e and 0.75 m_e, respectively.

Acknowledgements

We thank Dr T.F. Rosenbaum and Dr R. Xu for sending us their experimental results prior to publication and for beneficial discussions.

References

[1] R. Xu, A. Hussman, T.F. Rosenbaum, M.-L. Saboungi, J.E. Enderby, P.B. Littlewood, Nature 390 (1997) 57.
[2] I.S. Chuprakov, K.H. Dahmen, Appl. Phys. Lett. 72 (1998) 2165.
[3] Gmelins Handbuch der Anorganischen Chemie, Silber, band 3b (1973).
[4] P. Junod, Helv. Phys. Acta 32 (1959) 567.
[5] G.A. Wiegers, J. Less common Metals 48 (1976) 269.
[6] A. van der Lee, J.L. de Boer, Acta Cryst. C49 (1993) 1444.
[7] R. de Ridder, S. Amelinckx, Phys. Stat. Sol. (a) 18 (1973) 99.
[8] C. Kaito, N. Nakamura, T. Teraniski, S. Sakimoto, M. Shiojiri, Phys. Stat. Sol. (a) 71 (1982) 109.
[9] G.A. Wiegers, Am. Mineral 56 (1971) 1882.
[10] J.B. Conn, R.C. Taylor, J. Electrochem. Soc. 107 (1960) 977.
[11] H.M. Rietveld, Physico memo no. 153, Reactor Centrum Netherlands 1966.
[12] J. Rodriguez-Carvajal, FULLPROF, version 3.5, Dec. 1997, LLB-JRC.
[13] A.J. Frue, Am. Mineral. 44 (1959) 693.
[14] B.H. Tavernier, Z. Anorg. Allg. Chemie 343 (1966) 21.
[15] P. Messien, M. Baiwir, Bull. Soc. Royale Sciences Liege 35 (1966) 234.
[16] Johan, et al., Bull. Soc. Fr. Mineral. Cristallogr. 94 (1974) 381.
[17] T.J.M. Smit, E. Venema, J. Wiersma, G.A. Wiegers, J. Solid State Chem. 2 (1970) 309.
[18] H. van Leuken, A. Lodder, M.T. Czyzyk, F. Springelkamp, R.A. de Groot, Phys. Rev. B41 (1990) 5613.
[19] L. Hedin, B.I. Lundqvist, J. Phys. C 4 (1971) 2064.
[20] M.T. Czyzyk, R.A. de Groot, G. Dalba, P. Fornasini, K. Kisiel, F. Rocca, E. Burattini, Phys. Rev. B39 (1989) 9831.
[21] C.M. Fang, R.A. de Groot, Unpublished results.
[22] H. van Leuken, PhD thesis, Vrije Universiteit te Amsterdam, (1991).
[23] P. Junod, H. Hediger, B. Kichor, J. Wulischleger, Phil. Mag. 36 (1977) 941.
[24] V. Damodara, D. Karenakaran, Das, J. Appl. Phys. 67 (1990) 878.
[25] R.O. Jones, O. Gunnarsson, Rev. Modern Phys. 61 (1989) 689.
[26] S.A. Aliev, N.A. Verdieva, M.I. Aliev, Fiz. Tekh. Poluprovodh. 12 (1978) 2075.
[27] V.V. Gorbach, I.M. Putlin, Phys. Status Solidi B 69 (1975) K153.
[28] S.A. Aliev,, F.F. Aliev, Izv. Akad. Nauk SSSR, Neorgan. Mater. 21 (1978) 1869.
[29] R. Simon, R.C. Bushe, E.H. Lougher, Advanced Energy Conversion 3 (1963) 481.
[30] Z. Ogorelec, A. Hamzic, M. Basletic, Europhys. Lett. 46 (1999) 56.
[31] T. Thio, S.A. Solin, Appl. Phys. Lett. 72 (1998) 3497.
[32] T. Thio, S.A. Solin, J.W. Bennett, D.R. Hines, Phys. Rev. B57 (1998) 12239.
[33] A.A. Abrikosov, Phys. Rev. B58 (1998) 2788.